Chapter 1

Overview of Combustion Instabilities in Liquid-Propellant Rocket Engines

Fred E. C. Culick*
California Institute of Technology, Pasadena, California 91125
and
Vigor Yang†
Pennsylvania State University, University Park, Pennsylvania 16802

I. Introduction

COMBUSTION instabilities were discovered in solid- and liquid-propellant rocket engines at about the same time in the late 1930s. Since then, unstable oscillations have occurred in most, if not practically all, new development programs. Indeed, because of the high density of energy release in a volume having relatively low losses, conditions normally favor excitation and sustenance of oscillations in any combustion chamber intended for a propulsion system.

Figure 1 is an abbreviated chronology of some major events and features of the subject during the past 50 years. In one form or another, combustion instabilities have been under continuous study during all of that period. In time, however, the emphasis naturally has shifted, depending on what sort of full-scale systems experienced difficulties. During World War II in the United States, it seems that virtually all work in this subject was concerned with elimination of high-frequency resonant burning (the term used at the time) in small tactical solid rocket motors. The common treatment was usually a form of passive control, involving installation of baffles, resonance rods, or some other modification of geometry. Since then, the need to solve problems of instabilities in solid rockets has continued for motors of all sizes. Much of the basic understanding that has been gained is applicable to liquid rockets, despite the obvious differences in the systems.

Although work on combustion instabilities in liquid rockets began in the early 1940s, significant progress was neither achieved nor required until after World War II with the development of large intercontinental ballistic missiles (ICBMs). During the 1960s, the needs of the Apollo program motivated a large amount of work on instabilities, rendered particularly important because of the astronauts

*Professor of Mechanical Engineering and Jet Propulsion.

†Professor of Mechanical Engineering.

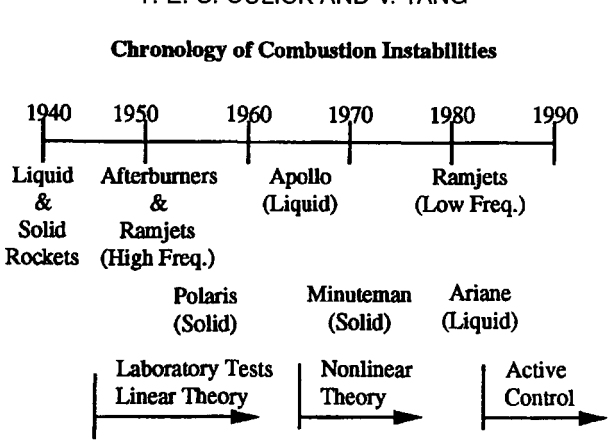

Fig. 1 Chronology of combustion instability.

onboard the rocket. That experience formed part of the basis for developing the Space Shuttle main engine. Practically no progress was made in the United States from the early 1970s to the middle 1980s, whereupon interest rose again with the prospects for developing the advanced launch system (ALS), which was subsequently canceled. In France, a small but significant program has been continuously supported since 1981 as part of the Ariane program. Chapters 4, 10, and 20 of this volume give most researchers in the West their first extensive acquaintance with the considerable body of work accomplished over many years in the former Soviet Union.

Combustion instabilities in jet-engine afterburners have been troublesome since the invention of these devices in the late 1940s. The types of problems encountered at that time still persist: high-frequency transverse modes, similar to the oscillations often found in liquid rockets. With the development of high-bypass engines, however, conditions became favorable for the entire length of the engine to participate in the motions, leading to the presence of longitudinal vibrations with lower frequencies that are much more difficult to treat simply by making changes in geometry.

Similarly, although earlier liquid-fueled ramjets had instabilities mainly in the high-frequency range, more compact designs in the late 1970s led to longitudinal oscillations having lower frequencies in the range of a few hundred hertz. Those problems received a great deal of attention during the 1980s, and several concentrated research programs have produced a quite good basic understanding of the causes and possible means of treatment.

Solid rockets also have exhibited instabilities over wide ranges of frequency, from the low frequencies arising in large ICBMs and strap-on booster rockets to very high frequencies in tactical solid rockets. Research on the problem in solid rockets has continued from the early 1950s to the present, at varying levels of intensity. Although in comparison with liquid rockets details of the problem (notably the basic causes) are significantly different in solid rockets, much of what has been learned about the general aspects of the problem is directly applicable to liquid rockets.

Indeed, quite generally, progress made in any one of these systems is relevant, and often importantly so, to understanding and treating combustion instabilities in other sorts of systems. This review of instabilities in liquid-propellant

rocket engines is brief, but nevertheless we shall often refer to results achieved in other systems as well, especially to encourage workers in the field to be aware of, if not conversant with, combustion instabilities in all types of propulsion systems.

To begin to understand the essential characteristics of combustion instabilities, it is best first to distinguish linear and nonlinear behavior. Linear behavior presents only one general problem, linear instability, which received widespread attention during the 1950s and 1960s; see, e.g., the monograph by Crocco and Cheng[1] and the comprehensive compilation of works edited by Harrje and Reardon.[2] Any disturbance may be synthesized as an infinite series of harmonic motions. An approximate analysis developed over many years (see Culick[3] and Culick and Yang[4]) allows one to use classical acoustic modes as the terms in the series and to compute the perturbations of the complex wave number for each mode due to various contributing processes in a combustion chamber. The real part of the wave number gives the frequency shift, and the imaginary part gives the growth (or decay) constant associated with each mode. Vanishment of the imaginary part determines the formal condition for linear stability, whose dependence on the parameters characterizing the system is then known.

Two basic nonlinear problems arise when dealing with combustion instabilities: determining the conditions for the existence and stability of limit cycles for a linearly unstable system and finding the conditions under which a linearly stable system may become unstable to a sufficiently large disturbance. In the language of modern dynamical systems theory, these two problems are identified as supercritical and subcritical bifurcations, respectively. The term bifurcation refers to the characteristic that the character of the steady behavior of the system suffers a qualitative change abruptly as a parameter of the system is varied continuously. This may at first seem an unnecessarily formal description of the phenomenon. In fact, the framework provided by the approximate analysis and application of some of the ideas of dynamical systems theory forms a widely useful and convenient basis for understanding combustion instabilities.

Figure 2 is a schematic diagram suggesting the commonly accepted point of view of combustion instabilities. A measurement of the pressure at a fixed location shows, roughly, a time dependence similar to that for the displacement of a simple mechanical oscillator. Hence, it is natural to suppose that the fluctuation of pressure

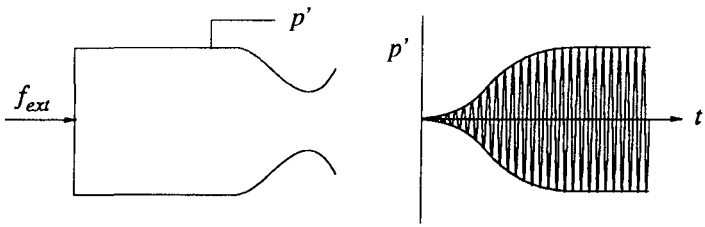

$$\frac{d^2p'}{dt^2} + 2\alpha\frac{dp'}{dt} + \omega_0^2 p' = f(t) = f_{int} + f_{ext}$$

$$p' = g(f) \Rightarrow f = g^{-1}(p')$$

Fig. 2 Pressure oscillations in a combustion chamber.

from its mean value satisfies the oscillator equation with damping constant α, natural frequency ω_0, and forcing $f(t)$,

$$\frac{d^2p'}{dt^2} + 2\alpha\frac{dp'}{dt} + \omega_0^2 p' = f(t) = f_{\text{int}} + f_{\text{ext}} \tag{1}$$

Usually there are no significant external forces acting on the flow in a combustion chamber: it is a good approximation to neglect f_{ext}. Then the internal force represents those processes not typically accounted for in α and ω_0, notably combustion and, in some formulations, nonlinear behavior.

For the moment, we confine attention to linear behavior exhibited as the exponentially growing amplitude in Fig. 2. It is convenient to assume that the terms $2\alpha\, dp'/dt + \omega_0^2 p'$ contain all linear processes except those associated with combustion. Thus, the internal forcing f_{int} contains the mechanisms tending to excite the instability. Although a priori determination of f_{int} is not always feasible, the following heuristic form may be assumed as a physically useful representation:

$$f_{\text{int}} = q(p') = 2\alpha_c\frac{dp'}{dt} + \omega_c^2 p' \tag{2}$$

With a view to later remarks on active control of combustion instabilities, we interpret the preceding model with the block diagram drawn in Fig. 3. The equation of motion, Eq. (1), is abbreviated by the relationship $p' = g(f)$ between the input (sum of internal and external forcing) and the output. The internal forcing (i.e., combustion response) depicted in Fig. 3 appears as a feedback path. Because the system is linear, the Laplace transform may be applied to represent the system in the frequency domain. The transfer function relating the pressure to the external force is

$$\frac{P(s)}{F_e(s)} = \frac{G(s)}{1 - Q(s)G(s)} \tag{3}$$

[Note that the force f_{int} is fed back positively to correctly represent the system defined by Eq. (1); hence, the minus sign, rather than the more familiar plus sign, appears in the denominator of Eq. (3).] The natural motions, possible when no external force is acting, are defined by equating the denominator of the transfer function to zero,

$$Q(s)G(s) - 1 = 0 \tag{4}$$

For the simple example here, with Eqs. (1) and (2) we find

$$G(s) = \frac{1}{s^2 + 2\alpha s + \omega_0^2} \qquad \text{and} \qquad Q(s) = 2\alpha_c s + \omega_c^2 \tag{5}$$

Substitution in Eq. (4) gives

$$s^2 + 2(\alpha - \alpha_c)s + \left(\omega_0^2 - \omega_c^2\right) = 0 \tag{6}$$

The roots of this equation are

$$s = -(\alpha - \alpha_c) \pm i\sqrt{\left(\omega_0^2 - \omega_c^2\right) - (\alpha - \alpha_c)^2} \tag{7}$$

Hence, as earlier argued, s has a possible positive real part, and the natural motion is unstable if $\alpha_c > \alpha$, assuming both α and α_c to be positive.

The condition $\alpha - \alpha_c = 0$ defines neutral stability; motions neither grow nor decay. When $\alpha - \alpha_c$ is expressed in terms of the parameters characterizing the system, the locus $\alpha - \alpha_c = 0$ in the space of parameters is called the stability boundary. In the literature of combustion instabilities, the stability boundary is normally computed in a quite different fashion but, as we shall see later, the results are equivalent.

A continuum, such as the gaseous environment inside a combustion chamber, is basically an infinite degree of freedom system. For time-harmonic behavior of the (linear) unsteady motions, however, the chamber boundary conditions allow solutions only at discrete modal frequencies. Each mode can basically be treated as a one-degree-of-freedom oscillator, demonstrating the utility of Eq. (1). It is well established that combustion response (i.e., the coefficients α_c and ω_c) varies with frequency. Therefore, the degree to which combustion destabilizes a mode depends on the frequency of the mode itself. If the energy gain due to combustion response is greater than energy damping, then an instability of the particular mode results. Mathematically, this condition is equivalent to having a positive real part of an eigenvalue in Eq. (7).

Although practical situations are profoundly more complex than the simplified system in Fig. 3, the preceding remarks summarize the basis for treating, and if possible eliminating, combustion instabilities in practice. Beginning with an unstable mode, there are clearly several ways to achieve the desired result that the modes should be stable. First, damping might be increased with the addition of attenuating devices, such as small resonant cavities or acoustic liners, a common practice in liquid-propellant rocket engines. This tactic will cause a small frequency shift, but a second method of stabilization involves changes of geometry to displace the resonant peaks sufficiently in frequency so that no peak is lower than the driving curve. That is one consequence of using baffles: breaking the chamber into effectively smaller compartments introduces new internal boundary conditions, causing the normal modes to occur at lower frequencies. On the other side of the energy balance, the strategy consists in reducing the driving in the vicinity of the unstable resonance. That is, generally, a more time-consuming and

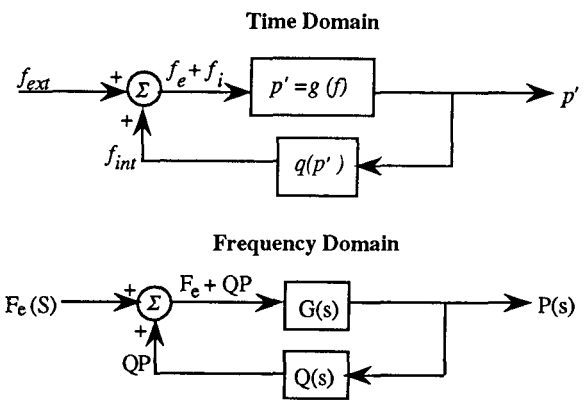

Fig. 3 Feedback loop of unsteady motions in a combustion chamber.

expensive procedure but is commonly a necessary approach when it is not possible to introduce sufficient damping to stabilize the system. Work to change injector design or the entry conditions of the injected propellants, in some sense never thoroughly understood, produces favorable effects on the driving curve.

The remainder of this chapter is divided into sections broadly summarizing the subjects covered in this volume. Following descriptions of several cases of instabilities, we briefly discuss the important fundamental processes generally recognized to be most significant in respect to combustion instabilities in liquid-propellant rocket engines. Numerical simulations and analysis are barely more than touched upon in Secs. IV and V. The crucially important practical matter of stability rating is reviewed in Sec. VI. A curious feature of the subject is that whereas data, but no theory, are available for stability rating (essentially the problem of nonlinear instability), theoretical results and relatively little data are available for linear stability. Thus, it is fair to state that research on combustion instabilities in liquid-propellant rocket engines has produced mainly formal theoretical results and a useful way of interpreting observations, but practically nothing of value for basic comparisons of theory and experiment. The most difficult problems of behavior found in operational systems remain unsolved by theory.

Section VII covers the very important subject of control. Only passive control has been applied to practical systems. Active control offers some promise for the future, but only after very substantial progress.

II. Two Examples of Combustion Instabilities in Operational Engines

In the preceding section, we have emphasized that distinguishing linear and nonlinear behavior produces one way of classifying combustion instabilities, particularly important for theoretical work. The distinctions between linear and nonlinear oscillations have also strongly influenced the planning and interpretation of experimental work. In some respects, a more immediately useful scheme to begin imposing order on the wide variety of observations is based on the propellants used. There are three main classes of propellants: liquid oxygen (LOX) with a hydrocarbon fuel, liquid oxygen and liquid hydrogen (commonly referred to as cryogenic propellants), and storable propellants, the most common being nitrogen tetroxide as the oxidizer and monomethylhydrazine (MMH) or A-50 [a mixture of 50% hydrazine, N_2H_4, and 50% unsymmetrical dimethylhydrazine (UDMH)] as the fuel. Since several chapters of this volume address many examples of combustion instabilities, we shall discuss briefly only two cases, both taken from the Apollo program: the first stage F-1 engine, which used propellants LOX/RP-1; and the lunar module descent engine (LMDE), which, of course, used storable propellants.

A. Combustion Instabilities in the F-1 Engine

The problem of instabilities in the F-1 engine was serious for more than seven years during development of the engine. Recently, Oefelein and Yang[5] presented a comprehensive review of the subject, the first such work based on a thorough study of the original reports and memoranda. Here, we shall give only a cursory discussion and a partial summary.

The F-1 engine was qualified for manned flight in 1966 to satisfy heavy-lift requirements of the Apollo program, but its origins can be traced back to several engines developed in the 1950s by Rocketdyne, principally the E-1; the Atlas

MA-2; and a derivative of the engine used in the Thor/Jupiter vehicle, the H-1, itself later used in Saturn I. Of the 44 tests of the first F-1 design carried out from January 1959 to May 1960, 20 experienced combustion instabilities with peak amplitudes greater than or comparable to the average pressure. This was contrary to predictions based on experimental and theoretical work at the time, and relatively poor instrumentation apparently provided little new useful information. The oscillations caused serious erosion and burning of the injector face, indicating the presence of large radial and tangential motions.

Distinctions between linear and nonlinear instabilities were recognized during the period 1960–1962 and, at least implicitly, helped guide the development of tests. In the literature of that time, the term self-triggering was often used to refer to spontaneous or linear instability, and dynamic instability meant that a linearly stable system was nonlinearly unstable to a sufficiently large disturbance. An important conclusion established by the early tests (1959–1962) and confirmed throughout subsequent work was that baffles were necessary to provide dynamic stability.

To circumvent the instability problems, a program called Project First was established to develop a stable F-1 engine. Project First lasted for four years and progressed in three steps: preliminary flight rating tests (PFRT), flight rating tests (FRT), and flight qualification tests. These stages ran from October 1962 to June 1963, June 1963 to January 1965, and January 1965 to September 1966, respectively, with the bulk of the work concerned with improving the injectors and the baffles. During this period, there were 207 full-scale tests with 11 injectors in PFRT, 422 tests with 46 injectors in FRT, and 703 tests with 51 injectors in the qualification program—a total of 1332 tests with 108 injectors. The F-1 engine from its beginning to flight was subject to more than 2000 full-scale tests, probably the most intensive (and expensive) program ever devoted primarily to solving a problem of combustion instabilities.

Figure 4 shows examples of the 5U injector with and without baffles. Iterations with respect to this pattern evolved into the flight qualified injector. Without baffles, the engine was prone to instabilities, a characteristic consistent with previous experience with engines using LOX/RP-1 as propellants. With a suitable combination of baffle configuration and injector design, the engine not only did not exhibit self-excited oscillations (linear instabilities) but was also stable to finite disturbances (nonlinear stability). Pressure records in the figure illustrate that behavior.

The report by Oefelein and Yang[5] provides details concerning the sequence of design changes made during the four years of Project First. What matters here are the main conclusions. For at least two reasons, longitudinal or organ-pipe modes tended to be more stable than tangential modes. First, the exhaust nozzle provides considerably more damping for longitudinal than for tangential modes; second, the physical and chemical processes near the injector face—containing practically all of the mechanisms producing instabilities—are generally more sensitive to velocity fluctuations parallel to the injector face than to unsteady motions normal to the face. Moreover, the velocity fluctuation near the head end is relatively small in a longitudinal wave, vanishing at a rigid end surface.

Several mechanisms for exciting instabilities are evidently active in the engine. The dominant ones seem to have been coupling between oscillations in the chamber and unsteady motions within the injection elements (injection coupling), periodic pulsed combustion of excess liquid-propellant accumulations on

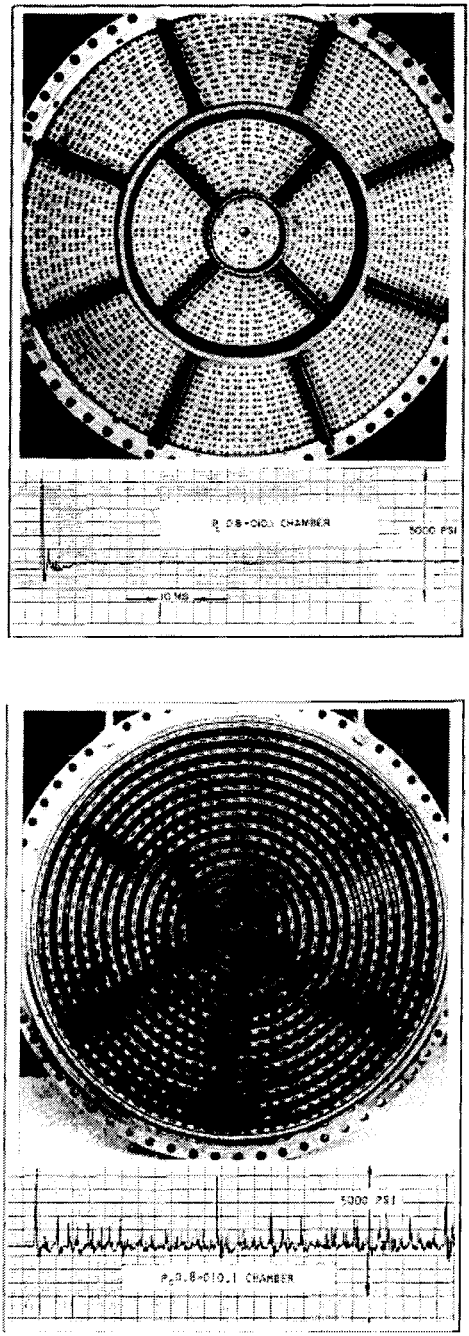

Fig. 4 Importance of baffles with respect to dynamic stability of F-1 engines.

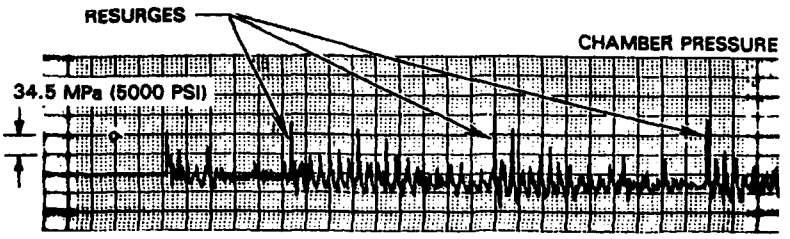

Fig. 5 Pressure trace exhibiting resurge phenomenon.

boundary surfaces accompanying film cooling, and transverse displacements of the injected fuel and oxidizer jets when exposed to oscillations of velocity parallel to the injector face. The first tangential mode was the troublesome oscillation, eventually subdued by a combination of modifications of the injector design and use of baffles extending downstream from the injector face.

Primary mechanisms responsible for instabilities in the F-1 engine were apparently located within three regions near the injector face and a fourth region associated with film cooling of surfaces. The last was identified with the dominant cause of a phenomenon called resurging, frequently observed following explosion of a bomb for rating dynamic stability. Figure 5 reproduces pressure traces showing resurging observed during the PFRT program. The dominant cause was pulsed combustion of liquid fuel detached from the liquid layer produced with the film cooling of the chamber. A secondary cause may have been rapid combustion of droplets at supercritical pressures. In any event, resurging was essentially eliminated by determining the best conditions of film cooling, the thickness of the film being the main parameter.

Whereas the mechanism associated with film cooling is largely specific to the injector design, other causes near the injector face are of much more general significance and remain the subject of research. The three regions referred to are 1) that nearest the injector face, containing the spray fans and all processes generating liquid drops of fuel, 2) the region of fuel vaporization extending roughly 10 in. downstream of the face; and 3) the region farther downstream in which both fuel and oxidizer are gaseous and where most of the combustion occurs. In the region closest to the injector, the dominant processes involve the dynamics of the liquid jets and the spray fans formed by impinging jets. Within this region, which extended roughly 3 in. from the injector face, formation of fuel droplets is nearly complete, and LOX drops were almost entirely vaporized. Note that the baffles finally used extended 3 in. downstream from the face, which had a diameter of 40 in. Hence, the baffles effectively shadowed the region in which interactions between jets and the processes forming the liquid drops are most important. A secondary consequence, whose importance was not quantified in the F-1 program, was the conversion of tangential fluctuations to longitudinal motions that are then damped by the action of the exhaust nozzle.[6] In region 2, fuel drops suffer breakup due to aerodynamic forces and are vaporized. It is here that vaporization is encouraged by the high relative velocity between gaseous oxygen and the liquid fuel drops. If the gaseous fuel and oxygen are not uniformly mixed as a result of the processes in regions 1 and 2, interactions with oscillations in the flow can cause fluctuations of the mixture ratio and, hence, of the burning rate. Interactions in region 3 highlighted the basic importance of the location of the combustion zone. Tests with design changes to produce larger fuel drops and higher relative velocity between

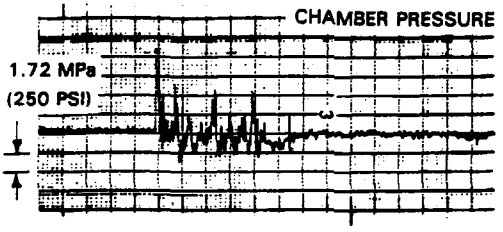

Fig. 6 Pressure trace exhibiting damping characteristics of FRT injector of F-1 engine.

the drops and the gaseous oxygen showed that the zone of vigorous burning moved downstream and improved stability. The final injector produced a specific impulse of 265.4 s and characteristic velocity efficiency equal to 93.8%, confirmed with 703 full-scale engine tests. Figure 6 shows test results typical of the behavior following bombing.

B. Combustion Stability of the Lunar Module Descent Engine

The Apollo LMDE operated with the storable propellants, N_2O_4 oxidizer and A-50 fuel. Owing to the stringent requirements for descent to landing on the moon, the engine had to be throttleable (ultimately over the range of 1000–9850 pounds thrust), with a maximum single firing time of 1000 s but with three starts required. Essentially, no combustion instability could be tolerated in the entire range of operation. The TR 201 engine,[7,8] conceived first by Elverum at the NASA Jet Propulsion Laboratory and later developed and produced by TRW, successfully met all of the requirements and remains one of the most remarkable liquid rocket engines ever used.

The general configuration of the engine and a sketch of the pintle injector are given in Chapter 5. Fuel is injected as a cylindrical tubular sheet along the axis, and oxidizer is injected radially as a number of jets near the end of the movable sleeve. On first acquaintance, one might expect this configuration to exhibit poor performance, but that is not the case. The specific impulse exceeds 300 s above 3000 pounds thrust. What is equally remarkable is that even during severe tests of dynamic stability by bombing, the engine "has never experienced a case of sustained high-frequency instability," a statement referring to the LMDE operated within its design envelope. The chief reason for the stability rests on the relative distributions of acoustic pressure and combustion energy release. Because of the way in which the liquid fuel and oxidizer are injected, the energy release tends to be most concentrated in an annular region between the axis and the chamber boundary and roughly midway between the head end and the nozzle. The central axial location is unfavorable to exciting the fundamental longitudinal mode (and, in fact, all odd modes), which is additionally highly damped by the exhaust nozzle. Moreover, the intermediate radial position has the least destabilizing influence on the first radial and first tangential modes.

In view of the remarks in the Introduction, one cannot expect an engine to be absolutely stable under all possible conditions. The TR 201 did show transient oscillations, particularly when rapidly throttled or at full thrust with a fuel-rich mixture or under some conditions of partial failure. Moreover, the envelope for

stable operation changes when different propellants are used. It is, however, fair to state that the engine is stable over a wide range of conditions for which it is qualified. The method of bombing to assess dynamic stability will be discussed briefly in Sec. VI.

III. Fundamental Processes

The purpose of the injection system and combustion chamber in a liquid rocket engine is to accomplish controllably the conversion of liquid propellants to product gases at high temperature and pressure. Thrust is then produced by expansion through the exhaust nozzle, transforming potential and thermal energy into kinetic energy. Although the characteristics of the flow in the nozzle are significant in determining the overall efficiency of the engine, we are concerned here chiefly with unsteady processes upstream of the nozzle entrance. The only significant contribution of the nozzle to combustion instabilities arises from its position, setting the downstream boundary conditions on waves in the chamber; its most important influence is attenuating longitudinal oscillations.

Figure 7 is a broad summary of the various elementary processes. It is convenient to display them in serial form, roughly corresponding to the sequence of events from propellant supply to exhaust. It is important, however, to realize that several different processes may take place simultaneously in a given region of space.

Several chapters in this volume provide good summaries of past work in this subject, the present state of understanding, and reports of research in progress. There is, therefore, no need here to dwell on details. We shall rather try to clarify the context within which the elementary processes may act as mechanisms for exciting and sustaining combustion instabilities. The discussion here, and in any consideration of fundamental processes, cannot be complete in a practical sense;

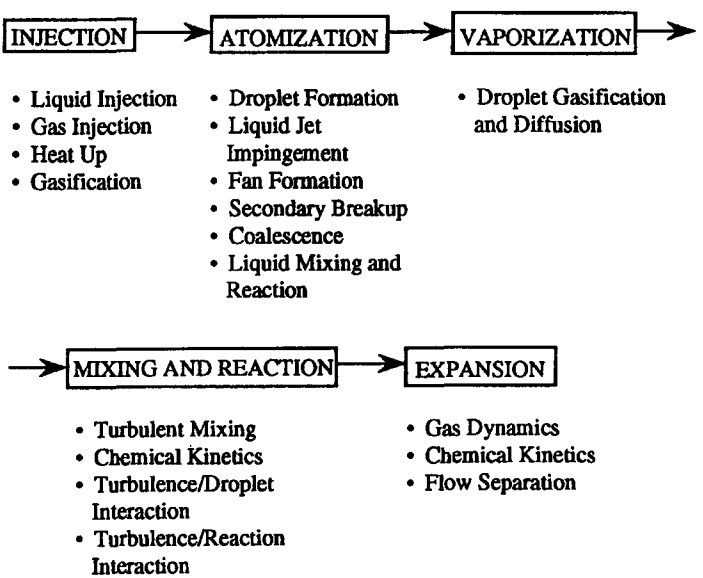

Fig. 7 Physicochemical processes involved in liquid rocket thrust chambers.

for a given engine, there are inevitably characteristics peculiar to the design. For example, we have seen in the case of the F-1 engine that accumulation of liquid fuel during film cooling of the chamber was responsible for an unacceptable spiking unsteady motion.

To bring some order to the possible importance of the many processes shown in Fig. 7, it is helpful to overlay a classification according to injector types.[9] For that purpose, we lump all possibilities into three classes distinguished by the configurations of the liquids when they are discharged by the injection elements into the chamber: 1) impinging jets, 2) concentric jets, and 3) jet/sheet (noncoaxial). The last class arises notably in the lunar descent module engine. Little is known about the fundamental processes involved in this type of pintle injector, although there is research in progress.

We have already discussed the F-1 engine using injectors based on impinging jets; other examples include the lunar ascent engine, several launch vehicles, and the Space Shuttle orbital maneuvering engine. Notable applications of concentric injectors include the RL-10 and the Space Shuttle main engine. In this volume, problems of impinging jets are discussed in Chapter 8 by Anderson and Santoro; concentric or coaxial injection processes are covered in Chapter 6 by Vingert et al., which includes an excellent review, and in Chapter 7 by Zaller and Klem. There seems to be no work which provides a basis for assessing quantitatively the relative stability of the various configurations. In this regard, there has been a suggestion that the Soviets regarded injectors with impinging jets as more prone to causing combustion instabilities than those using coaxial jets, even with hydrocarbon fuels. We have been unable to verify that conclusion.

Figure 8, taken from Ref. 10, is a photograph showing one type of situation for a case of impinging liquid jets. Immediately following impingement, a spray fan or sheet is formed. Either because of disturbances already growing in the jets or because the sheet is itself unstable (possibly for both reasons), the sheet breaks up. There are several forms of the breakup but, in any event, a cloud of liquid drops or droplets is formed having a fairly broad distribution of size and velocity. Because of the surrounding atmosphere of moving gases, the sheet and the drops are subject to shear forces that encourage breakup of both. In a combustion chamber, these processes take place in an atmosphere consisting of combustion product gases and reactant gases as well.

The greater part of what is known about the events in which liquid jets are transformed to drops has come from tests with liquids at room temperature and with no combustion. Whereas it is true that such tests are necessary, valuable, and do produce a great deal of useful information, one must never forget that the situation may be drastically different when combustion occurs. Heat transfer upstream and pressure disturbances generated by combustion of individual drops may have strong effects on the jets and spray sheets before and during breakup. For example, with hypergolic propellants, blow-a-part of the reactive streams and popping or intermittent explosion of liquid may be sufficiently vigorous to excite instabilities.

Whatever the environment, the first step in the transformation of liquid jets to drops must involve some sort of instability. For the case of impinging jets, the jets themselves may be unstable, or the spray fan is unstable. Concentric jets are unstable at their interface. The basic processes responsible for the instabilities are characterized by various dimensionless groups that provide scaling laws (see Chapters 6 and 9 for particularly good discussions of scaling).

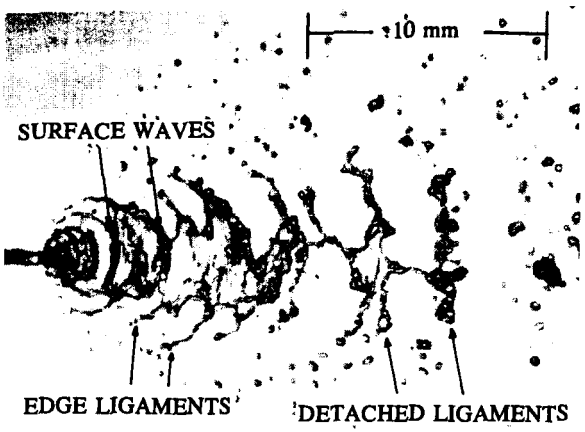

Fig. 8 Typical spray formed by two turbulent impinging water jets.

Determining the distributions of drop size and velocity theoretically is an extremely difficult problem, more so than the matter of incipient instability. In general, the influences of aerodynamic forces on the breakup of jets and the secondary breakup of drops is so complicated as to be beyond realistic analysis.

Combustion occurs in the gaseous phase and must be preceded by mixing. In a LOX/hydrocarbon system, such as in the F-1, vaporization of the liquid oxygen occurs much more rapidly than that of the liquid fuel. Hence, a significant part of the spray combustion involves vaporization and subsequent combustion of the fuel in an oxygen-rich atmosphere. It appears that some of the consequences of detailed design changes on the injector elements may be explained ultimately by the large difference in vaporization rates. That characteristic must also have much to do with differences in the stability of concentric injectors compared with impinging jets when the same propellant combination is used.

Whereas burning of single drops has been actively studied for many decades and is quite well understood (see Chap. 11 by Sirignano et al. for details), spray combustion, particularly for dense clouds of interacting drops under conditions found in a rocket combustion chamber, is poorly understood. Only ad hoc modeling is available for unsteady combustion of sprays. In addition to the purely fluid-mechanical and chemical problems, serious further complications arise in combustion chambers operated at high pressure, namely, those arising from behavior in the supercritical regime. This is not a new subject, but thorough analysis for conditions appropriate to combustion instabilities in liquid rocket engines is recent and unfinished.[11-14] The fundamental origin of the special behavior accompanying combustion near the critical point is the rapid variations of thermophysical properties. For a given substance or mixture of substances, the critical properties are well defined. However, the special characteristics of behavior at the critical point itself extend, albeit attenuated, into some region around the critical point. Hence, it is clearly unnecessary for the chamber conditions to be precisely at the critical state to cause unusual phenomena during combustion.

To be specific, consider a liquid drop of oxygen injected as liquid (and hence having a temperature below the critical point) into a hot fuel-rich environment—the simplest case being hot hydrogen. Suppose that the chamber pressure is greater

than the critical value for some mixture of the fuel and oxidizer. As the drop follows its trajectory, its temperature rises, oxygen vaporizes, and gaseous hydrogen diffuses inward. Somewhere between the center of the drop and the environment far away, the temperature and pressure may, if conditions are suitable, assume the critical values for the local mixture ratio of oxygen and hydrogen. For a spherically symmetric flow, the critical point is reached on a spherical surface. Locally, the sharp variations of properties with temperature will produce drastic changes in the flowfield at and near that surface. Globally, those effects have a substantial influence on the vaporization rate.

If oscillations of pressure and temperature occur in the environment, then it is possible, even though the average chamber pressure may be far from critical, that critical conditions are reached in some point of the drop under unsteady conditions. Then transient fluctuations can be amplified by the large fluctuations of thermodynamic properties. The result is a new possibility for coupling between acoustical motions in the chamber and droplet burning. The most thorough analysis of droplet vaporization and combustion under supercritical conditions has been covered in recent publications in Refs. 11–14. As the preceding remarks suggest, calculations in which supercritical behavior is ignored are seriously in error when the chamber pressure is greater than the critical states of the injected propellants.

IV. Analysis and Numerical Simulations

As in many fields of engineering, the rapidly increasing power of computing resources continues to motivate increasingly elaborate calculations of unsteady behavior in combustion chambers. The term numerical simulation refers to numerical solution to the governing equations of motion, comprising the fundamental conservation equations and models of all physical processes included in the formulation. There are two sorts of inaccuracies in numerical simulation: computational errors and those arising from approximations in the equations. The numerical analysis itself cannot be perfect, although for most applications contemporary methods have practically negligible errors in their range of validity. Modeling the physical processes is necessarily imperfect and is by far the main reason for inaccurate results. Thus, even with the remarkable progress in computing power, it is still not realistic to attempt to solve fully three-dimensional, time-dependent problems for combustion chambers; both the modeling of combustion processes and available computing power are inadequate.

Other than the unavoidable limitations just discussed and the expenses involved, the main disadvantage of numerical simulation is that each case computed is just that: one case. Understanding global behavior and trends over the possible ranges of parameters defining a given problem can be extremely expensive and time consuming and often does not lead to clear, simple rules useful for interpreting experimental data and for practical design. Hence, there will always be a need for formal analysis, which must in any event be approximate.

An approximate analysis must be founded on the same governing equations as a numerical simulation, but commonly with some simplifications in models of the physical processes, to help gain solutions. Hence for a given problem, numerical simulations should be at least as accurate as analytical results. The great advantages of an approximate analysis are the possibility for deducing general rules and the opportunity to investigate theoretically the global behavior of a complicated system. For the subject of combustion instabilities, the most important use of the second characteristic is in understanding nonlinear behavior.

Thus, the entire subject of combustion instabilities may be viewed as divided into three parts: experiments and full-scale tests, analysis and theory, and numerical simulations, sometimes also viewed as a part of computational fluid dynamics (CFD). The case of the F-1 engine discussed in Sec. II is an (perhaps, the) extreme example of how expensive a problem of combustion instabilities can be in a development program. Probably the chief practical purpose of both analysis and numerical simulations is to provide a sound basis for reducing the amount of experimentation and testing required. It will never be possible to eliminate testing entirely, but theoretical work can achieve a great deal by narrowing the ranges of parameters that must be covered in tests.

In this section we first describe briefly the general formulation and modeling used presently for investigating combustion instabilities in liquid rocket engines. We then summarize one form of approximate analysis that has proved effective in other applications and for deriving some useful theoretical results. It is unnecessary here to cover numerical simulations that are treated quite thoroughly in this volume in Chapter 18 by Habiballah and in Chapter 19 by Grenda et al.

A. Equations for Unsteady Motions in Combustion Chambers

We shall neither derive equations of motion here nor deal with the most general forms. Our chief purpose is to convey as thoroughly as possible the main ideas and to outline the basis for the more important theoretical results. Even though the instabilities observed are mainly oscillations of the gaseous phase, it is essential to account for the presence of the liquid phase as well. To simplify the discussion, we lump the liquid fuel and oxidizer together as a single liquid phase and represent the multicomponent gas mixture as a single average gas.[3,4] Thus, we treat a reacting two-phase mixture for which the equations of conservation are as follows.

Conservation of mass:

$$\frac{\partial}{\partial t}(\rho_g + \rho_\ell) + \nabla \cdot (\rho_g \boldsymbol{u}_g + \rho_\ell \boldsymbol{u}_\ell) = w_{eg} + w_{e\ell} \tag{8}$$

Conservation of momentum:

$$\frac{\partial}{\partial t}(\rho_g \boldsymbol{u}_g + \rho_\ell \boldsymbol{u}_\ell) + \nabla \cdot (\rho_g \boldsymbol{u}_g \boldsymbol{u}_g + \rho_\ell \boldsymbol{u}_\ell \boldsymbol{u}_\ell) = \nabla \cdot \tau_g + \boldsymbol{m}_{eg} + \boldsymbol{m}_{e\ell} \tag{9}$$

Conservation of energy:

$$\begin{aligned} &\frac{\partial}{\partial t}(\rho_g e_{g_0} + \rho_\ell e_{\ell_0}) + \nabla \cdot (\rho_g \boldsymbol{u}_g e_{g_0} + \rho_\ell \boldsymbol{u}_\ell e_{\ell_0}) \\ &\quad = \nabla \cdot (\tau_g \cdot \boldsymbol{u}_g) - \nabla \cdot \boldsymbol{q}_g + Q + Q_e \end{aligned} \tag{10}$$

Subscript g refers to the gas species and subscript ℓ to the liquid; subscript 0 denotes the stagnation state. External sources are denoted by subscript e. These terms do not normally appear in the literature but are included here because they may be used to represent the presence of active control, a subject to be addressed later. Stress tensor τ_g is assumed to depend on properties of the gas phase and may be written as the sum of the isotropic pressure and the viscous stress tensor τ_v,

$$\tau_g = -p\boldsymbol{I} + \tau_v \tag{11}$$

All forces exerted in the flow by external influences are represented by the momentum sources $\boldsymbol{m}_{eg}$ and $\boldsymbol{m}_{e\ell}$. Distributed forces (gravity, electromagnetic, etc.) are not an issue in the problems considered here; nonzero values of $\boldsymbol{m}_{eg}$ and $\boldsymbol{m}_{e\ell}$ will arise due to momentum transfer associated with flow of material through the boundary of the combustion chamber and interactions associated with material injected for actuating control. Internal heat flow is represented by $\boldsymbol{q}_g$, sufficiently well approximated by Fourier's law for the gas phase; Q represents heat addition in the gas phase associated with combustion processes not accompanying conversion of the condensed phase to gas. Hence, the symbol e_{g_0} stands for stagnation thermal energy only, containing no part related to chemical processes. For a mixture of perfect gases, each species having constant specific heat,

$$e_{g_0} = C_v T_g + \tfrac{1}{2} u_g^2 \tag{12}$$

where C_v and u_g strictly stand for values mass averaged over all gaseous species.

Let w_ℓ denote the rate at which the liquid phase is converted to gas, and Eq. (8) can be written as the sum of the following two equations.

Conservation of mass (gas phase):

$$\frac{\partial \rho_g}{\partial t} + \nabla \cdot (\rho_g \boldsymbol{u}_g) = w_\ell + w_{e_g} \tag{13}$$

Conservation of mass (liquid phase):

$$\frac{\partial \rho_\ell}{\partial t} + \nabla \cdot (\rho_\ell \boldsymbol{u}_\ell) = -w_\ell + w_{e\ell} \tag{14}$$

The following manipulations are directed to eventually writing a nonlinear wave equation governing the behavior of waves in the mixture. Elasticity (the spring constant) for wave propagation is provided by the compressibility of the gas only, whereas the mass of an elementary oscillator in the medium is the sum of the masses of gas and liquid in a unit volume.

Equation (8), the equation for the total density of the mixture, can be rewritten as

$$\frac{\partial \rho}{\partial t} + \nabla \cdot (\rho \boldsymbol{u}_g) = \mathcal{W} + \mathcal{W}_e \tag{15}$$

where $\rho = \rho_\ell + \rho_g$, the total external source of mass is

$$\mathcal{W}_e = w_{eg} + w_{e\ell} \tag{16}$$

and

$$\mathcal{W} = -\nabla \cdot (\rho_\ell \delta \boldsymbol{u}_\ell) \tag{17}$$

The slip velocity between the condensed phase and the gas is defined as $\delta \boldsymbol{u}_\ell = \boldsymbol{u}_\ell - \boldsymbol{u}_g$. Now expand the momentum equation (9) and substitute the definitions to give the following.

Conservation of momentum (gas phase):

$$\rho_g \frac{\partial \boldsymbol{u}_g}{\partial t} + \rho_g \boldsymbol{u}_g \cdot \nabla \boldsymbol{u}_g + \nabla p = \nabla \cdot \tau_v + \boldsymbol{F}_\ell - (\sigma + \sigma_e - \boldsymbol{m}_e) \tag{18}$$

where

$$\boldsymbol{F}_\ell = -\rho_\ell\left[\frac{\partial \boldsymbol{u}_\ell}{\partial t} + \boldsymbol{u}_\ell \cdot \nabla \boldsymbol{u}_\ell\right] \tag{19}$$

$$\sigma = (\boldsymbol{u}_g - \boldsymbol{u}_\ell)w_\ell = -\delta \boldsymbol{u}_\ell w_\ell \tag{20}$$

$$\sigma_e = \boldsymbol{u}_g w_{eg} + \boldsymbol{u}_\ell w_{e\ell} \tag{21}$$

$$\boldsymbol{m}_e = \boldsymbol{m}_{eg} + \boldsymbol{m}_{e\ell} \tag{22}$$

Equation (19) is the momentum equation for the condensed phase, and σ represents the rate at which momentum is supplied to the newly created gas phase by the gases already present. Hence $-\sigma$ in Eq. (18) represents the force exerted on the gas phase by the vaporizing condensed phase.

To Eq. (18) add $\rho_\ell[\partial \boldsymbol{u}_g/\partial t + \boldsymbol{u}_g \cdot \nabla \boldsymbol{u}_g]$ to find

$$\rho\left[\frac{\partial \boldsymbol{u}_g}{\partial t} + \boldsymbol{u}_g \cdot \nabla \boldsymbol{u}_g\right] + \nabla p = \nabla \cdot \tau_v + \delta \boldsymbol{F}_\ell - (\sigma + \sigma_e - \boldsymbol{m}_e) \tag{23}$$

where

$$\delta \boldsymbol{F}_\ell = -\rho_\ell\left[\frac{\partial \delta \boldsymbol{u}_\ell}{\partial t} + \delta \boldsymbol{u}_\ell \cdot \nabla \delta \boldsymbol{u}_\ell + \delta \boldsymbol{u}_\ell \cdot \nabla \boldsymbol{u}_g + \boldsymbol{u}_g \cdot \nabla \delta \boldsymbol{u}_\ell\right] \tag{24}$$

is the force of interaction between the condensed and gas phases.

More elaborate manipulations eventually lead to the energy equation for the temperature of the gas phase,

$$\begin{aligned}\rho \bar{C}_v\left[\frac{\partial T_g}{\partial t} + \boldsymbol{u}_g \cdot \nabla T_g\right] + p\nabla \cdot \boldsymbol{u}_g \\ = (\tau_v \cdot \nabla)\boldsymbol{u}_g - \nabla \cdot \boldsymbol{q}_g + (Q + Q_e) + \boldsymbol{u}_g \cdot (\sigma + \sigma_e - \boldsymbol{m}_e) \\ + \delta Q_\ell + w_\ell \delta e_0 + \delta \boldsymbol{u}_\ell \cdot \boldsymbol{F}_\ell - (e_{g_0} w_{eg} + e_{\ell o} w_{e\ell})\end{aligned} \tag{25}$$

where

$$Q_\ell = -\rho_\ell\left[\frac{\partial e_\ell}{\partial t} + \boldsymbol{u}_\ell \cdot \nabla e_\ell\right], \qquad \text{and} \qquad \delta e_0 = e_{\ell_0} - e_{g_0} \tag{26}$$

Corresponding to Eq. (24), the heat exchange between the two phases is

$$\delta Q_\ell = -\rho_\ell C_\ell\left[\frac{\partial \delta T_\ell}{\partial t} + \delta \boldsymbol{u}_\ell \cdot \nabla \delta T_\ell + \delta \boldsymbol{u}_\ell \cdot \nabla T_g + \boldsymbol{u}_g \cdot \nabla \delta T_\ell\right] \tag{27}$$

where $\delta T_\ell = T_\ell - T_g$. The mass-averaged specific heat for the mixture is defined as

$$\bar{C}_v = \frac{1}{\rho}(\rho_g C_v + \rho_\ell C_\ell) = \frac{C_v + C_m C_\ell}{1 + C_m} \tag{28}$$

and $C_m = \rho_\ell/\rho$ is the liquid-phase loading, the fraction of mass in unit volume as liquid.

To simplify writing, we shall hereafter use the symbol $\boldsymbol{u}$ instead of $\boldsymbol{u}_g$ for the gas velocity, T instead of T_g for the gas temperature, and drop the overbars on mass-averaged thermodynamic properties. Thus, the three basic equations for unsteady motions in a two-phase mixture are as follows.

Conservation of mass:

$$\frac{\mathrm{D}\rho}{\mathrm{D}t} = -\rho\nabla\cdot\boldsymbol{u} + \mathcal{W} + \mathcal{W}_e \tag{29}$$

Conservation of momentum:

$$\rho\frac{\mathrm{D}\boldsymbol{u}}{\mathrm{D}t} = -\nabla p + \mathcal{F} + \mathcal{F}_e \tag{30}$$

Conservation of energy:

$$\rho C_v\frac{\mathrm{D}T}{\mathrm{D}t} = -p\nabla\cdot\boldsymbol{u} + \mathcal{Q} + \mathcal{Q}_e \tag{31}$$

where the sources are

$$\mathcal{W} + \mathcal{W}_e = -\nabla\cdot(\rho_\ell\delta\boldsymbol{u}_\ell) + w_{eg} + w_{e\ell} \tag{32}$$

$$\mathcal{F} + \mathcal{F}_e = \nabla\cdot\tau_v - \sigma + \delta\boldsymbol{F}_\ell - (\sigma_e - \boldsymbol{m}_e) \tag{33}$$

$$\begin{aligned}\mathcal{Q} + \mathcal{Q}_e = {} & (\tau_v\cdot\nabla)\boldsymbol{u} - \nabla\cdot\boldsymbol{q}_g + Q + \boldsymbol{u}\cdot\sigma_e + \delta Q_\ell + \delta e_0 w_\ell + \delta\boldsymbol{u}_\ell\cdot\boldsymbol{F}_\ell \\ & + \boldsymbol{u}\cdot(\sigma_e - \boldsymbol{m}_e) - \left(e_{g_0}w_{e_g} + e_{\ell_0}w_{e_\ell}\right) + Q_e\end{aligned} \tag{34}$$

The substantial derivative is defined in terms of the gas velocity,

$$\frac{\mathrm{D}}{\mathrm{D}t} = \frac{\partial}{\partial t} + \boldsymbol{u}\cdot\nabla \tag{35}$$

The equation of state appropriate to this formulation is

$$p = \rho R T_g \tag{36}$$

where R is the mass-averaged gas constant, equal to $\bar{C}_p - \bar{C}_v$. From the preceding equations, the equation for the pressure can be derived,

$$\frac{\mathrm{D}p}{\mathrm{D}t} = -\gamma p\nabla\cdot\boldsymbol{u} + \mathcal{P} + \mathcal{P}_e \tag{37}$$

with

$$\mathcal{P} + \mathcal{P}_e = \frac{R}{C_v}Q - RT\nabla\cdot(\rho_\ell\delta\boldsymbol{u}_\ell) + p\frac{\mathrm{D}\ell_n R}{\mathrm{D}t} + \left(\frac{R}{C_v}Q_e + RTw_e\right) \tag{38}$$

Equations (29–31) and the equations of state (36) describe the motions of the two-phase mixture. With the possibility of small modifications or extensions to accommodate many species, these are the basic equations for all analyses of combustion instabilities. To obtain solutions, in addition to setting boundary conditions, the condensed phase must be treated separately with Eqs. (14), (19),

and (27), with suitable laws for the force and heat exchange between the two phases.

We shall not pursue the matter of properly posed problems, a subject addressed in this volume in those chapters dealing with numerical simulations. Moreover, although the equations derived here can be used as the basis for nonlinear analysis, we shall restrict ourselves here to a short outline of linear stability analysis that will serve sufficiently well for later discussion of some special topics. A comprehensive discussion of nonlinear oscillations in rocket engines is given in Chapter 13 of this volume.

B. Wave Equation and Approximate Solution

A wave equation may be constructed by analogy with a procedure followed in classical acoustics. Because nonlinear behavior will not be treated herein, we shall work from the beginning with the linearized forms of the governing equations. Write all variables as sums of mean and fluctuating parts, $p = \bar{p} + p'$, etc., and assume that the mean values are independent of time. Substitute in Eqs. (30) and (37) and ignore terms of second order and higher in the fluctuations to find

$$\bar{\rho}\frac{\partial \boldsymbol{u}'}{\partial t} = -\bar{\rho}(\bar{\boldsymbol{u}} \cdot \nabla \boldsymbol{u}' + \boldsymbol{u}' \cdot \nabla \bar{\boldsymbol{u}}) - \nabla p' + \mathcal{F}' + \mathcal{F}_e' \tag{39}$$

$$\frac{\partial p'}{\partial t} = -\gamma \bar{p} \nabla \cdot \boldsymbol{u}' - \gamma p' \nabla \cdot \bar{\boldsymbol{u}} - \bar{\boldsymbol{u}} \cdot \nabla p' + \mathcal{P}' + \mathcal{P}_e' \tag{40}$$

We have also assumed that the mean pressure and density are uniform. Now differentiate Eq. (40) with respect to time, substitute Eq. (39), and rearrange the result to find

$$\nabla^2 p' - \frac{1}{\bar{a}^2}\frac{\partial^2 p'}{\partial t^2} = h + h_e \tag{41}$$

where

$$h + h_e = -\bar{\rho}\nabla \cdot (\bar{\boldsymbol{u}} \cdot \nabla \boldsymbol{u}' + \boldsymbol{u}' \cdot \nabla \bar{\boldsymbol{u}}) + \frac{1}{\bar{a}^2}\bar{\boldsymbol{u}} \cdot \nabla \frac{\partial p'}{\partial t}$$
$$+ \frac{\gamma}{\bar{a}^2}\frac{\partial p'}{\partial t}\nabla \cdot \bar{\boldsymbol{u}} + \nabla \cdot \mathcal{F}' - \frac{1}{\bar{a}^2}\frac{\partial \mathcal{P}'}{\partial t} + \nabla \cdot \mathcal{F}_e' - \frac{1}{\bar{a}^2}\frac{\partial \mathcal{P}_e'}{\partial t} \tag{42}$$

Terms identified by subscript e always correspond.

The boundary condition is set on the normal gradient of the pressure by taking the scalar product of Eq. (39) with the outward normal vector $\boldsymbol{n}$, giving

$$\boldsymbol{n} \cdot \nabla p' = -f - f_e \tag{43}$$

where

$$f + f_e = \bar{\rho}\frac{\partial \boldsymbol{u}'}{\partial t} \cdot \boldsymbol{n} + \bar{\rho}(\bar{\boldsymbol{u}} \cdot \nabla \boldsymbol{u}' + \boldsymbol{u}' \cdot \nabla \bar{\boldsymbol{u}}) \cdot \boldsymbol{n} - \mathcal{F}' \cdot \boldsymbol{n} - \mathcal{F}_e' \cdot \boldsymbol{n} \tag{44}$$

The first term f is commonly rewritten by introducing a response or admittance function characterizing the unsteady behavior of the boundary in response to imposed fluctuations.

Only gasdynamical interactions between the mean and fluctuating velocity fields are shown explicitly in Eqs. (41–44). All other processes are hidden in $\mathcal{P}'$ and $\mathcal{F}'$, those directly associated with external (control) actions being contained in $\mathcal{F}_e'$ and $\mathcal{P}_e'$.

Traditional calculations of linear behavior are based on the differential equations (39) and (40), augmented by the linearized equation of state and possibly by linearized forms of other equations given in Sec. IV.A. In the remainder of this chapter we will use the integrated form based on spatial averaging described, for example, by Culick and Yang.[4] The fundamental idea is that the actual problem defined by Eq. (41) with its boundary condition, Eq. (43), differs in some sense by small amounts from the classical acoustics problem defined by setting $h = f = h_e = f_e = 0$. That is, the influences of all processes are small perturbations. This formulation, then, has the form naturally suited to an iteration procedure readily constructed by introducing a Green's function as first accomplished by Culick.[15] However, the identical first-order result (the only order legitimately considered with these equations) is obtained more directly in the following way.

The unperturbed problem defines the normal modes, with mode shapes ψ_n and natural frequencies $\omega_n = \bar{a}k_n$, where k_n is the wave number,

$$\nabla^2\psi_n + k_n^2\psi_n = 0 \tag{45}$$

$$\boldsymbol{n}\cdot\nabla\psi_n = 0 \tag{46}$$

The idea is then to compare the perturbed (actual) and unperturbed (classical) problems quite literally by comparing their difference in a spatially averaged sense. Multiply Eq. (41) by ψ_n, Eq. (45) by p', and subtract and integrate over the volume of the chamber to give

$$\int \left[\psi_n\nabla^2 p' - p'\nabla^2\psi_n\right] dV$$

$$-\frac{1}{\bar{a}^2}\int\left[\psi_n\frac{\partial^2 p'}{\partial t^2} - \omega_n^2 p'\psi_n\right] dV = \int \psi_n(h + h_e)\, dV$$

Upon application of Green's theorem and substitution of the boundary conditions, Eqs. (43) and (46), we find

$$\frac{1}{\bar{a}^2}\int\psi_n\left[\frac{\partial^2 p'}{\partial t^2} + \omega_n^2 p'\right] dV = -\left[\int \psi_n h\, dV + \oiint \psi_n f\, dS\right]$$

$$-\left[\int \psi_n h_e\, dV + \oiint \psi_n f_e\, dS\right] \tag{47}$$

The preceding calculations are formally correct and introduce no errors. Now we make the approximation that the pressure field in the actual chamber can be expanded in a series of normal modes for the classical unperturbed problem,

$$p' = \bar{p}\sum_{n=1}^{\infty}\eta_n(t)\psi_n(\boldsymbol{r}) \tag{48}$$

The error incurred in the results arises because $\psi_n(\boldsymbol{r})$, and therefore the right-hand side, do not satisfy the correct boundary condition (43) set on p' in the actual problem. When the series is used in the given integrals, the error is attenuated, and for other formal reasons not covered here (see, e.g., Morse and Feshback[16]) the use of Eq. (48) is entirely legitimate. The inaccuracy is not as serious an inaccuracy as one might think. We assume also, not a practical constraint, that the normal modes are orthogonal,

$$\int \psi_m \psi_n \, \mathrm{d}V = E_n^2 \delta_{mn} \tag{49}$$

Substitution in Eq. (47) leads finally to the second-order equations for the amplitudes $\eta_n(t)$,

$$\frac{\mathrm{d}^2 \eta_n}{\mathrm{d}t^2} + \omega_n^2 \eta_n = F_n + F_{ne} \tag{50}$$

and the forcing terms are

$$F_n = -\frac{\bar{a}^2}{\bar{p} E_n^2} \left\{ \int h \psi_n \, \mathrm{d}V + \oiint f \psi_n \, \mathrm{d}S \right\} \tag{51}$$

$$F_{ne} = -\frac{\bar{a}^2}{\bar{p} E_n^2} \left\{ \int h_e \psi_n \, \mathrm{d}V + \oiint f_e \psi_n \, \mathrm{d}S \right\} \tag{52}$$

With proper interpretation and suitable modeling of the processes represented in functions h, f, h_e, and f_e, the representation of combustion instabilities by Eqs. (50–52) has wide applications to all propulsion systems. Relatively little has been done with this formulation applied specifically to liquid rocket engines but, as we shall see shortly, it is quite easy to obtain general results equivalent to those obtained with methods more familiar in this field.

An important point to emphasize is that the approach taken here provides a useful viewpoint as well as a framework useful for both theoretical and practical computations. According to Eqs. (48) and (50), any unsteady motion may be regarded as a collection of oscillators, one associated with each normal mode of oscillation appearing in the synthesis, Eq. (48). The problem then comes down to determining the time evolution of the amplitudes $\eta_n(t)$ of the oscillators (modes). Although we have assumed linear motions here, the same formal representation applies to nonlinear motions, so long as the amplitudes do not become so large as to violate the approximations taken to give the governing differential equations.

V. Some Results of Analysis

The point has been emphasized that with the analysis involving spatial averaging, as constructed in the preceding section, we can accommodate practically any process active in real combustion. Of course, some approximations are involved, and it is necessary to work out explicit representations or models of the processes in question, but the situation is quite different from that which arises when one chooses to solve the partial differential equations governing the motion. In that case, numerical solutions accentuate errors in modeling because of the differentiation required. Moreover, it is easier with the framework available here to discuss

quite general results in a relatively simple and clear fashion. With a few exceptions, we will not be concerned with detailed examples in the remainder of this chapter.

A. Linear Stability

As remarked earlier, there is really only one problem of linear stability, and it is readily solved within the present analysis. According to the principles of Fourier analysis, with essentially no practical restrictions, any function can be synthesized as a finite or infinite series of orthogonal functions. Here, we apply the idea to a pressure record represented as a sum of the normal modes $\psi_n(\boldsymbol{r})$ of a chamber, with time-dependent amplitudes $\eta_n(t)$, Eq. (48). Finding the normal modes requires solving the classical problem of the scalar wave equation for a closed volume that has the same shape as the combustion chamber in question, with the exception that the exhaust nozzle is closed at its entrance. Both the mode shapes $\psi_n(\boldsymbol{r})$ and the natural frequencies are found in this calculation, the solution to Eqs. (45) and (46).

For the problem of linear stability, the amplitudes are assumed to have the form

$$\eta_n(t) = \hat{\eta}_n e^{i\bar{a}K_n t} \tag{53}$$

where the actual complex wave number is

$$K_n = (\Omega_n - i\alpha_n)/\bar{a} \tag{54}$$

Now the perturbed mode corresponding to the nth classical mode may either grow ($\alpha_n > 0$) or decay ($\alpha_n < 0$) in time. The actual frequency is

$$\Omega_n = \omega_n + \delta\omega_n \tag{55}$$

Hence, the problem of linear stability comes down to determining the frequency shift $\delta\omega_n$ and growth constant α_n for each perturbed mode. The basis for the calculation is the linearized form of the equations already treated.

Substitute Eqs. (53–55) in Eq. (50), with $F_{ne} = 0$ to find*

$$(\Omega_n - i\alpha_n)^2 = \omega_n^2 - \hat{F}_n/\hat{\eta}_n$$

where, for linear behavior, we write $h = \hat{h}e^{i\bar{a}K_n t}$ and $f = \hat{f}e^{i\bar{a}K_n t}$, so that $F_n = \hat{F}_n e^{i\bar{a}K_n t}$. For the usual case, $\alpha_n \ll \Omega_n$ and $(\Omega_n - \omega_n)/\omega_n \ll 1$, which must be satisfied to be consistent with approximations already made. Then separating the real and imaginary parts of the last equation, with the definition (51), gives

$$\Omega_n = \omega_n + \frac{\bar{a}^2}{2\omega_n \bar{p} E_n^2}\left\{\int \frac{\hat{h}^{(r)}}{\hat{\eta}_n}\psi_n \, dV + \oiint \frac{\hat{f}^{(r)}}{\hat{\eta}_n}\psi_n \, dS\right\} \tag{56}$$

$$\alpha_n = \frac{-\bar{a}^2}{2\omega_n \bar{p} E_n^2}\left\{\int \frac{\hat{h}^{(i)}}{\hat{\eta}_n}\psi_n \, dV + \oiint \frac{\hat{f}^{(i)}}{\hat{\eta}_n}\psi_n \, dS\right\} \tag{57}$$

*The result and therefore Eqs. (56) and (57) are obtained only if no linear coupling of modes is contained in Eqs. (51) and (52) after the expansion (48) and the corresponding representation of the velocity fluctuation have been substituted. Linear coupling can be formally eliminated by constructing a new set of orthogonal modes. However, normally the corrections will contribute only higher order terms in Eqs. (56) and (57), and so no error is committed by simply ignoring linear coupling throughout the analysis.

in which superscripts (r) and (i) denote real and imaginary parts. These two formulas are the solution to the problem of linear stability. In particular, setting $\alpha_n = 0$ defines the stability boundary in terms of the various parameters arising in the functions h and f. That result is the basis for the Standard Stability Prediction Program[17] written for the U.S. Air Force and widely used by industrial and governmental organizations to analyze the stability of unsteady motions in solid propellant rockets.

B. Rayleigh's Criterion

Probably the most widely quoted general principle in the field of combustion instabilities is the criterion formulated by Rayleigh in 1878[18,19]:

> If heat be periodically communicated to, and abstracted from, a mass of air vibrating (for example) in a cylinder bounded by a piston, the effect produced will depend upon the phase of the vibration at which the transfer of heat takes place. If heat be given to the air at the moment of greatest condensation, or be taken from it at the moment of greatest rarefaction, the vibration is encouraged. On the other hand, if heat be given at the moment of greatest rarefaction, or abstracted at the moment of greatest condensation, the vibration is discouraged.

Roughly, the gist of the principle is that heat addition tends most strongly to drive acoustic waves if the energy is added in the region of space where the oscillating pressure reaches greatest amplitude and is in phase. Although the principle seems fairly obviously true, these remarks do not serve as proof. The formulation described can be used not only to establish the criterion but also to extend its application to all processes and nonlinear behavior as well.[3,20] Zinn[21] has recently discussed Rayleigh's criterion but only for linear heat addition.

We take advantage of the fact that each acoustic mode has an associated oscillator having unit mass and natural frequency ω_n, whose motion (i.e., time evolution of its amplitude η_n) is described by Eq. (50). The energy of a simple oscillator is the sum of its kinetic and potential energies,

$$\mathcal{E}_n = \tfrac{1}{2}(\dot{\eta}_n^2 + \omega_n^2 \eta_n^2) \tag{58}$$

We interpret Rayleigh's criterion to be a statement concerning the change $\Delta\mathcal{E}_n$ of the energy in one cycle. The product of the force $(F_n + F_{ne})$ times the velocity $\dot{\eta}_n$ is the power input, and so

$$\Delta\mathcal{E}_n(t) = \int_t^{t+\tau_n} (F_n + F_{ne})\dot{\eta}_n \, dt' \tag{59}$$

In general, $\Delta\mathcal{E}_n(t)$ varies with time, increasing from cycle to cycle for an unstable mode.

Indeed, for linear motions, if all processes are taken into account, $\Delta\mathcal{E}_n$ is proportional to the growth constant α_n, and this extended form of Rayleigh's criterion is equivalent to the principle of linear stability,[3,4]

$$\Delta\mathcal{E}_n = 2\pi\omega_n\alpha_n \tag{60}$$

Consequently, the precise form of Rayleigh's stated criterion is found by taking only the part of F_n that represents heat addition and setting $F_{ne} = 0$. The result is[20]

$$\Delta\mathcal{E}_n(t) = (\gamma - 1)\frac{\omega_n^2}{\bar{p}E_n^2}\int \psi_n \, dV \int_t^{t+\tau_n} \eta_n Q' \, dt' \tag{61}$$

in which Q' must be expressed in terms of real quantities. Thus, instead of the complex form we write in the case Q' proportional to p',

$$Q' = Q_0\psi_n(\beta_1\eta_n + \beta_2\dot{\eta}_n) \tag{62}$$

where β_1 and β_2 are real. The formula (61) leads to

$$\Delta\mathcal{E}_n = \pi(\gamma - 1)\beta_1\omega_n Q_0 \tag{63}$$

Thus, $\Delta\mathcal{E}_n$ is positive if $\beta_1 Q_0 > 0$, requiring that some portion of the heat addition must be in phase with the pressure fluctuation, as stated by Rayleigh.

Combination of Eqs. (60) and (61) gives the convenient formula for the growth constant due to heat addition,

$$\alpha_n = \frac{(\gamma - 1)\omega_n}{2\pi\bar{p}E_n^2}\int \psi_n \, dV \int_t^{t+\tau_n} \eta_n Q' \, dt' \tag{64}$$

where we have used the fact that $\eta_n Q'$ has period $\tau_n = 2\pi/\omega_n$ to shift the limits of the integral. We should also note that whereas the time derivative $\partial Q'/\partial t$ appears as the source in the wave equation (41) and in the oscillator equations (50), Q' itself occurs in Eqs. (61) and (64), also as a consequence of periodicity as explained by Culick.[20]

C. Response Factors

Particularly during the time when a great deal of effort was being devoted to problems of combustion instabilities in engines intended for the Apollo vehicle, the notion of a response factor was frequently applied. Although the various definitions used may differ in detail, the essential idea is common to all: a response factor is a quantity whose numerical value is a measure of the destabilizing effect of a process whose behavior is approximated by a linear model. It appears that all definitions of response factors are equivalent to the definition of the growth (or decay) constant α_n given by formula (57) through the approximate analysis formulated in Sec. IV. The interpretation of α_n follows from its definition and the definition of the energy in an acoustic wave. For small amplitude motions, the energy per unit volume is the sum of kinetic and potential energies,

$$\tfrac{1}{2}\rho(u')^2 + \tfrac{1}{2}(p')^2/\rho \tag{65}$$

To the approximation required in this analysis, $\boldsymbol{u}'$ and p' can be replaced by their classical, unperturbed relations; for the nth mode,

$$p_n' = \bar{p}\hat{\eta}_n e^{(i\omega_n + \alpha_n)t}\psi_n; \qquad \boldsymbol{u}_n' = i\frac{\bar{p}}{\bar{\rho}}\frac{\hat{\eta}_n}{\omega_n}e^{(i\omega_n + \alpha_n)t}\nabla\psi_n \tag{66}$$

The total time-averaged energy in the chamber is

$$\langle \mathcal{E}_n \rangle = \frac{1}{\tau_n} \int_t^{t+\tau_n} dt' \int dV \left[\frac{1}{2} \bar{\rho} (\mathrm{Re}\{\boldsymbol{u}_n'\})^2 + \frac{1}{2} \frac{(\mathrm{Re}\{p_n'\})^2}{\bar{\rho}} \right] \tag{67}$$

Substitution of Eq. (66) and carrying out the integrals gives

$$\langle \mathcal{E}_n \rangle = \mathcal{E}_{n0} e^{2\alpha_n t} \tag{68}$$

where $\mathcal{E}_{n0}$ is a constant. Hence,

$$\alpha_n = \frac{1}{2} \frac{1}{\langle \mathcal{E}_n \rangle} \frac{d\langle \mathcal{E}_n \rangle}{dt} \tag{69}$$

is half of the fractional rate of change of the time-averaged energy in the mode.

Since it is a result for linear behavior, the formula (57) for α_n is a sum of terms on the right-hand side, with each term being associated with a single process. For example, consider only the first term in f on the right-hand side of Eq. (44) and ignore all others in $h + h_e$ and $f + f_e$; then Eq. (57) becomes

$$\alpha_n = \frac{-\gamma}{2\omega_n E_n^2} \oiint \frac{1}{\hat{\eta}_n} \left(\frac{\partial \hat{\boldsymbol{u}}'}{\partial t} \cdot \boldsymbol{n} \right)^{(i)} \psi_n \, dS \tag{70}$$

where the superscript caret means taking the factor multiplying $e^{i\omega_n t}$. It is common practice in acoustics to represent the response of a surface with an admittance function A. Here, that model implies assuming that the velocity normal to the surface induced by an imposed pressure fluctuation is proportional to that fluctuation,

$$\boldsymbol{u}' \cdot \boldsymbol{n} = A(\bar{a}/\bar{p}) p' \tag{71}$$

where the ratio $\bar{a}/\bar{p}$ has been introduced to make A dimensionless. [Note that $\boldsymbol{n}$ is positive outward. A negative sign should be added to the definition of the admittance function if $\boldsymbol{u}$ is positive inward. See Ref. 4 for a thorough discussion.] Because $A = A^{(r)} + iA^{(i)}$ is complex, it follows that

$$\begin{aligned} \frac{\partial \boldsymbol{u}'}{\partial t} \cdot \boldsymbol{n} &= (A^{(r)} + iA^{(i)}) \frac{\bar{a}}{\bar{p}} \frac{\partial p'}{\partial t} \\ &\approx (A^{(r)} + iA^{(i)})(\bar{a}/\bar{p}) i\omega_n \hat{\eta}_n \psi_n e^{i\omega_n t} \end{aligned}$$

and

$$\left(\frac{\partial \hat{\boldsymbol{u}}'}{\partial t} \cdot \boldsymbol{n} \right)^{(i)} = (\bar{a}/\bar{p}) \omega_n A^{(r)} \hat{\eta}_n \psi_n$$

The formula (70) becomes

$$\alpha_n = \frac{-\gamma \bar{a}}{2\bar{p} E_n^2} \oiint A^{(r)} \psi_n^2 \, dS \tag{72}$$

This is a familiar result; with the definition of the growth constant used here, α_n is negative (stabilizing) if the real part of the admittance function is positive. Moreover, those parts of the surface contribute most where the mode shape has

the greatest amplitude. These conclusions amount to a Rayleigh's criterion for the response of a surface.

Similar special formulas can be deduced for processes in volume. Each formula for a contribution to the net growth constant is proportional to a response factor whose form depends on the definitions chosen. A response method, then, consists generally in computing the various response factors and summing the results. In short, a response method is entirely equivalent to a computation of linear stability that, as we have shown in the preceding section, amounts to the most general form of Rayleigh's criterion.

D. Time Lag (n, τ) Representation

Shortly after oscillations were encountered in early tests of liquid-propellant rocket engines in the United States, von Kármán suggested representing the mechanism with a time lag.[22] The idea was also independently introduced by Gunder and Friant[23] in 1950 and was subsequently developed to the greatest degree possible by Crocco and his students at Princeton; see Ref. 1 for thorough coverage of the subject.

The essential idea is that a finite interval—the time lag—exists between the time at which an element of propellant enters the chamber and the time at which it burns and releases its chemical energy. Such a lag must always exist, and there is no unique value because combustion is distributed throughout the chamber. If the pressure has the time dependence $p' = \bar{p}\psi_n(\boldsymbol{r}) \sin \omega_n t$, then the simplest way to introduce a time lag is to assume that the fluctuation of energy release has the form

$$Q' = \hat{Q}(\boldsymbol{r}) \sin \omega_n (t - \tau) \tag{73}$$

where τ represents the time lag. Substitution in the form of Rayleigh's criterion, Eq. (61), gives

$$\begin{aligned} \Delta \mathcal{E}_n &= 2\pi \omega_n \alpha_n \\ &= (\gamma - 1) \frac{\omega_n^2}{\bar{p} E_n^2} \int \psi_n(\boldsymbol{r}) \hat{Q}(\boldsymbol{r}) \, \mathrm{d}V \int_t^{t+\tau_n} \sin \omega_n t' \sin \omega_n (t' - \tau) \, \mathrm{d}t' \end{aligned} \tag{74}$$

and α_n is

$$\alpha_n = (\gamma - 1) \frac{1}{2\bar{p} E_n^2} \int \psi_n(\boldsymbol{r}) \hat{Q}(\boldsymbol{r}) \, \mathrm{d}V \cos \omega_n \tau \tag{75}$$

If $\hat{Q}$ is itself proportional to the local pressure amplitude ψ_n, then the integral is positive, and α_n is positive if $0 < \omega_n \tau < \pi/2, 3\pi/2 < \omega_n \tau < 5\pi/2, \ldots$. The process is destabilizing if τ is in the ranges of

$$0 < \tau < \frac{\pi}{2\omega_n}; \qquad \frac{3\pi}{2\omega_n} < \tau < \frac{5\pi}{2\omega_n}; \qquad \cdots \tag{76}$$

Although the oscillating behavior of α_n given by Eq. (75) is not in any sense fundamentally unacceptable, many examples of attempts to infer time lags for real processes suggest that such a result is unrealistic.[24,25] Part of the difficulty comes

from the assumption usually made (in the absence of other information) that the time lag is independent of frequency. Even on intuitive grounds, one should expect that behavior is not the case. In at least one case for the response of a burning solid propellant, both theory and experiment show that any time lag introduced to represent the behavior must depend significantly on frequency.

It appears that all applications of the time-lag model are based on the reasoning[1,3] given by Crocco. The principal result is the formula for the fluctuation of conversion of liquid to gas, the source term in the continuity equations (13) and (14),

$$w'_\ell = \bar{w}_\ell n\left[\frac{p'(t)}{\bar{p}} - \frac{p'(t-\tau)}{\bar{p}}\right] \tag{77}$$

where the interaction index n represents the sensitivity of propellant combustion to pressure oscillation. No details of physical processes are treated in the construction of this result, although of course they are implied in the definitions of n and τ. To analyze linear stability, assume that a single mode is present and that $p' = \bar{p}\hat{\eta}_n e^{i\omega_n t}\psi_n(\boldsymbol{r})$, $w'_\ell = \hat{w}_\ell e^{i\omega_n t}$ to give

$$\hat{w}_\ell = \bar{w}_\ell n(1 - e^{-i\omega_n\tau})\hat{\eta}_n\psi_n(\boldsymbol{r}) \tag{78}$$

It is perhaps best to interpret Eq. (78) as a particular two-parameter representation of the complex function $\hat{w}_\ell$. The real and imaginary parts of the formula are

$$\hat{w}_\ell^{(r)} = n\bar{w}_\ell(1 - \cos\omega_n\tau)\hat{\eta}_n\psi_n(\boldsymbol{r}), \qquad \hat{w}_\ell^{(i)} = n\bar{w}_\ell \sin(\omega_n\tau)\hat{\eta}_n\psi_n(\boldsymbol{r}) \tag{79}$$

Formally, the $(n-\tau)$ model simply replaces the two functions $\hat{w}_\ell^{(r)}$ and $\hat{w}_\ell^{(i)}$ with the two quantities n and τ. There is some advantage in having even a crude understanding of the physical basis for this form. Any advantage is lost if the model is taken too seriously without recognizing its serious limitations, the chief one being the fact that n and τ are not constant in reality and, thus, the serious uncertainties in w'_ℓ are not clarified by simply introducing n and τ.

There have been successful applications of the idea, notably in laboratory experiments at Princeton reported by Crocco et al.[26] and as a means of correlating extensive data taken in some development programs during the 1960s.[2] The way in which the results (78) or (79) are used in applications can be explained very simply with formulas we have derived with the approximate analysis. With the external contributions dropped, the general formulas (56) and (57) for linear stability are

$$\Omega_n = \omega_n - \frac{1}{2\omega_n}\left(\frac{\hat{F}_n}{\hat{\eta}_n}\right)^{(r)} \tag{80}$$

$$\alpha_n = \frac{1}{2\omega_n}\left(\frac{\hat{F}_n}{\hat{\eta}_n}\right)^{(i)} \tag{81}$$

It is a simple matter to trace the contribution of the mass source w_ℓ from Eq. (79) to Eqs. (51) and (52). Obviously, there will be a term linear in the fluctuation w'_ℓ; in fact, it is $\partial w'_\ell/\partial t$ that appears so that the term in $\hat{F}_n$ is proportional to $i\hat{w}_\ell$. The

details are unimportant here; the essential point is that Eqs. (80) and (81) take the form

$$\Omega_n = \omega_n + C_3 \int \psi_n \hat{w}_\ell^{(i)} \, dV - C_4 \tag{82}$$

$$\alpha_n = C_1 \int \psi_n \hat{w}_\ell^{(r)} \, dV - C_2 \tag{83}$$

On the stability boundary, $\alpha_n = 0$, and after substitution of Eq. (79), we can write the two formulas for the two unknowns n and τ:

$$n \sin \omega_n \tau = \left[(\Omega_n - \omega_n + C_4) \Big/ \left(C_3 \int \psi_n^2 \bar{w}_\ell \, dV \right) \right] \tag{84}$$

$$n(1 - \cos \omega_n \tau) = \left(C_2 / C_1 \int \psi_n^2 \bar{w}_\ell \, dV \right) \tag{85}$$

The right-hand sides are functions of the parameters defining the system according to injector type, geometry, dominant processes, and so forth. In practice, the idea is to vary those parameters and find the loci of values in such a way that small changes in one direction produce unstable oscillations and that changes in the other direction (i.e., to the other side of the locus) cause small disturbances to be attenuated. Then the right-hand sides of Eqs. (84) and (85) are known on the stability boundary, and the two equations can be solved for n and τ. Further discussion and some results may be found in the early work by Crocco et al.[26] and in Ref. 2.

It may at times be useful to introduce the n–τ model providing its limitations are understood, but the time has passed when this should be a major part of any analysis of combustion instabilities. With the increasing growth of large numerical simulations, any serious need for the n–τ model is rapidly disappearing. Money, time, and effort are now much better spent on more fundamental investigations of the processes actually present in an engine.

VI. Stability Rating

As interesting and challenging as understanding combustion instabilities is, the eventual purpose in practice is to guarantee their nonexistence. Theory, analysis, and laboratory work should establish the basic laws governing unsteady behavior, that is, scaling laws—dependence on geometry and other parameters that define the system, generally representing as thoroughly as possible linear and nonlinear behavior. If the task could be carried out to completion, then the basis would exist for minimum development costs of stable engines, with test programs planned mainly to confirm expected performance and stability. The actual case is still far from the ideal, and important testing procedures devised to establish stability characteristics of engines remain an important—and expensive—part of any development program. Such procedures define the process called stability rating.

As is the case for much of this subject, Ref. 2 remains the most complete reference for stability. Little seems to have changed in the past 20 years except for improvements in instrumentation, data acquisition, and data processing. Although other methods have been used to investigate special aspects of stability (e.g., oscillations involving the propellant supply system), here we shall

discuss briefly only the two basic methods used routinely to determine the stability of high-frequency wave modes in a chamber. Bombing a chamber by initiating small explosive charges, the older of the two, was introduced in the 1950s. The second method is called temperature ramping in which the temperature of one of the propellants, usually the fuel, is increased more or less linearly in time until an unstable motion develops spontaneously, or, less commonly, the transient following a small explosion becomes a sustained oscillation. Because ample guidance is available elsewhere for applying these methods, there is no need here for elaborating details. Rather, only a general context with examples is provided.

We have emphasized that there are two general kinds of stability, linear and nonlinear. Stability rating in the linear sense means determining the stability boundary in some space of parameters. For example, when the n–τ model of unsteady combustion is used, the essential parameters are, of course, n and τ. As explained in Sec. V.D, however, the values of n and τ can only be inferred as functions of parameters that can be controlled experimentally, e.g., oxidizer-fuel ratio or geometrical properties of the chamber. Determining n and τ from experimental work requires a model, normally that producing Eq. (77), and a linear stability theory that gives, for example, relations such as Eqs. (84) and (85). Thus, the procedure is truly semiempirical, based on a mixture of theoretical and observational results. As used in engine development, methods of stability rating do not appeal to any theoretical results. A limited number of parameters are changed (e.g., explosive charge size or propellant temperature), and the stability of motions is then assumed in some simple terms, such as rate of decay or growth of oscillations. Frequency shifts are normally small, or cannot be interpreted meaningfully, so that the best one can do in rating linear stability is to determine the rate of growth or decay.

Nonlinear stability is intrinsically a far more difficult matter than linear stability. There is no satisfactory, comprehensive theory for nonlinear combustion instabilities even though much is known in respect to the stability of nonlinear dynamical systems in general. Nonlinear instability means that a linearly stable system becomes unstable to a sufficiently large disturbance. We are concerned here with systems that contain sources and sinks of energy. The problem of nonlinear instability is, therefore, not simply an elaboration of the motion of a rotating pendulum in a gravitational field; in that case, small initial disturbances produce small-amplitude to-and-fro oscillations but sufficiently large disturbances cause the pendulum to execute continuing circular motions.

For rocket engines, the only practical means of assessing nonlinear stability is based on detonating small explosive charges. A typical strategy involves a sequence of charges, increasing in size to reach a condition at which the disturbance no longer decays but continues as more-or-less periodic large-amplitude motions. Empirical rules have been constructed to define what constitutes acceptable dynamic stability of a chamber.

VII. Passive and Active Control of Combustion Instabilities

The ultimate practical purpose of studying combustion instabilities is to develop sufficient understanding to be able to control the amplitudes at acceptable levels. Quite generally, there are only two strategies to follow: change the basic design of the system (geometry, injector type, etc.) or introduce some sort of control. Because constraints set for other reasons often prevent sufficient changes in design, much

effort has necessarily been exerted to devise means of control, always by passive means in operational propulsion systems.

A. Passive Control

The term "passive control" applies to the installation of baffles, resonators, or acoustic liners that suppress acoustic waves in the chamber. The essential point is to force the resonance to occur in frequency ranges where the driving mechanisms are inadequate to sustain oscillations or to directly damp the mechanical energy of unsteady motions. A secondary, but potentially more significant reason for the effectiveness of baffles, remarked upon in connection with the F-1 engine in Sec.II.A, is the possibility for shadowing regions of sensitive processes from disturbances. Figure 4 illustrates the idea that radial baffles extending axially into the chamber cause certain modes to be suppressed. A single baffle placed along a diameter, for example, will discourage spinning modes. These symmetrically placed radial baffles act against tangential oscillations. The effectiveness of baffles is limited by the practical constraint that they cannot extend too far from the injector face because structural integrity may be sacrificed and flow losses may be unacceptable.

Whatever the device used, limitations always arise because of its frequency response. Resonators may be the most obvious example, typically showing a fairly narrow peaked response whose height is reduced and width is increased for larger amplitude motions. Although the data on the behavior of passive devices taken in scale models at room temperature is inexpensive to acquire and usually serves as a useful guide in design, care must be exercised when extrapolating these results to practical rocket engines due to the differences in temperature and associated speed of sound. The performance of these devices is most conveniently expressed directly as an attenuation constant or, if more detailed behavior is known, an impedance or admittance function may be defined and used in a formula such as Eq. (72).

B. Active Control

Active control of combustion instabilities has received considerable attention in the past 10 years even though it is not a new concept. Tsien[27] suggested that the chugging instability in a liquid rocket motor could be stabilized by controlling the supply of propellant. Figure 9 is a sketch explaining his proposal. The main item is a feedback control loop based on sensing the pressure and controlling the line capacitance. The system may be modeled with the simple analysis outlined in Sec. IV. With a time-lag model of combustion, Eq. (1) becomes

$$\frac{\mathrm{d}^2 p'}{\mathrm{d}t^2} + 2\alpha \frac{\mathrm{d}p'}{\mathrm{d}t} + \omega_0^2 p' = \beta p'(t-\tau) + u(t) \tag{86}$$

where $u(t)$ is the control force. In the chugging mode, the chamber pressure is practically uniform so that p' here, indeed, represents the pressure measured everywhere. Taking the Laplace transform of Eq. (86), we find the relation between the transform $P(s)$ of the pressure and that of the control force $U(s)$

$$P(s) = [G/(1 - GQ)]U(s) \tag{87}$$

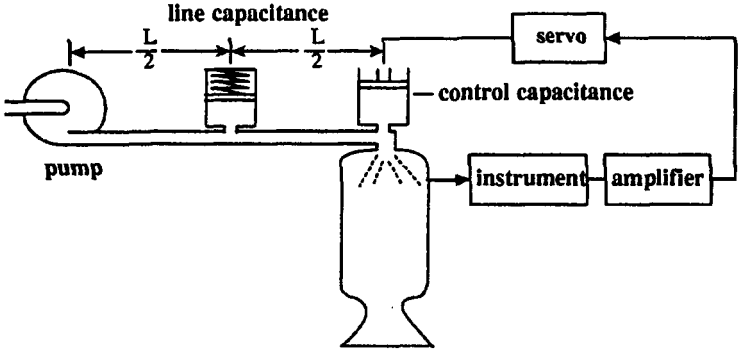

Fig. 9 Feedback control of chugging instability.

where G is the transfer function of the chamber (or the plant in the terminology of control theory),

$$G(s) = 1/(s^2 + 2\alpha s + \omega_0^2) \tag{88}$$

and

$$Q = \beta e^{-s\tau} \tag{89}$$

The result (87) has exactly the form interpreted with the block diagram drawn in Fig. 3. Well-known methods of classical control theory may be applied to investigate the performance and stability of this feedback system, although things are complicated somewhat by the presence of the time lag.

Tsien's method[27] of active control has never been successfully applied in practice. When it was first proposed, the available instrumentation and transducers were likely inadequate. Subsequently, the problem of chugging, most familiar in the form of the POGO instability, has been satisfactorily solved by passive control in operational systems.

Contemporary ideas of active control began about 10 years ago as an outgrowth of the field of noise control. A common and successful method of noise control is based on the idea of antisound[28] in which destructive interference is caused by injecting an appropriate acoustic field to cancel unwanted noise. Almost all demonstrated applications of active control have been based on that idea. Culick has provided a brief review of the work through 1988 in Ref. 3. Similar work has continued, largely associated with the development of air-breathing engines such as afterburners and gas-turbine combustors.

As emphasized earlier, the analysis described in Sec. IV has a form that is naturally adapted to the application of modern control theory. In the control field, the subject is called control of distributed systems. The source terms denoted by subscript e in the analysis accommodate any practical means of control, including actions in the chamber and at the boundary. The only systematical work on the control of combustion instabilities based on this approach appears in Fung[29] and in associated publications.[30–32]

In this context, any analysis of active control begins with the set of coupled oscillator equations (50). The theoretical work is then divided into two main parts: modeling the dominant physical processes and designing a controller. The most difficult part of the problem is the modeling, which by necessity

also includes modeling the actuators used. Combustion systems offer especially challenging problems in this respect because they are intrinsically nonlinear and contain substantial noise, and the activity of control changes the characteristics of the plant being controlled. Another way of expressing the last point is that there are inevitably uncertainties in the value of the parameters characterizing the plant.

If linear behavior is assumed, and the system has been satisfactorily modeled, then the available methods of modern control theory can be applied. It is a much more difficult matter if nonlinear processes are taken into account. For practical applications, the most serious obstacle is probably actuation. There seems to be general agreement that if active control is to succeed with operational systems, actuation will likely involve control of the propellant supply. The few results available were obtained with gas-filled laboratory devices. Control with liquid propellants is evidently much more difficult, with no successes reported.

A fundamental reason for difficulties of controlling the propellant supply, and therefore combustion processes, is the lack of understanding of the internal processes: modeling is again a central problem. It is likely that significant time lags are unavoidable; indeed, time lags are probably variable and non-uniform in space. Whereas active control of combustion instabilities seems to be a promising approach, success with large-scale systems is by no means assumed. Much research remains to be accomplished.

VIII. Concluding Remarks

Most of the progress in the area of combustion instabilities in liquid rocket engines was achieved prior to the early 1970s. Although there have been some notable advances since then, there has been relatively little change in basic understanding. This is the case partly because there has been no pressing need for a large, vigorous, and continuing research program that involves both theory and experiment. A significant exception has been the ONERA work in France, begun in 1981 as a result of flight failures of the Ariane vehicle. The relatively modest size of the program has probably limited the rate of accomplishments, but the sustained effort is unique in the field.

As in virtually all fields of terrestrial fluid mechanics, any successful research effort must comprise three parts: experiment, theory, and numerical simulation (CFD). The rocket propulsion community has generally been slow to take advantage of the rapid advances in computing resources and computational fluid mechanics, but that situation has been changing in the past several years. Some of the chapters in this volume summarize recent progress and suggest what is possible in the near future.

It is essential in a thorough investigation of combustion instabilities that all relevant driving and damping processes be accounted for. Stability depends on the balance of energy gains and losses; no matter how attractive a particular mechanism may appear, a proper conclusion can be reached only in the context of a framework treating all aspects of the problem. Experimental results, of course, necessarily contain all physical and chemical processes. Computing resources have advanced to the stage at which most relevant processes can be included in numerical simulations.

More traditional analysis, such as that outlined in this chapter, remains a central part of the basis for interpreting experimental results, understanding observed

behavior, and for theoretical work. There is a broad spectrum of problems to be treated, having many applications in combustion devices generally. It is fundamentally important that analytical work be integrated as thoroughly as possible with numerical simulations and experimental results. Purely theoretical work in this field is practically impossible. The problems are so complicated that analysis must be motivated by observations and, as we have emphasized in the introductory remarks, it is a fruitful strategy to incorporate from the beginning certain global aspects of observed behavior and then develop an analysis. Numerical simulations are in that respect closer to a level of proceeding directly from first principles. Therefore, an important role for numerical simulations is to provide a basis for assessing the validity of approximate results. Accurate confirmation leads to confidence in extending the analysis to situations for which numerical simulations are prohibitively expensive.

There is presently a large mismatch between available theories and experimental results. Theoretical and analytical results for linear behavior are the most advanced. Indeed, for all practical purposes, one might argue that linear theory is now complete. That is not to claim that highly accurate results can be obtained because many processes are still imperfectly understood; modeling is inaccurate, and necessary ancillary data are often uncertain as well. Even though the basic theory is well understood, there are relatively few experimental results available to check the theory in detail.

On the other hand, the greater part of observational data have to do with nonlinear behavior for which the theory is in a very primitive state. Particularly outstanding in this regard is the matter of nonlinear instability, the general characteristic that is investigated with the experimental technique called bombing. Nearly 30 years have passed since Crocco and his students first began treating nonlinear behavior, yet there is really no practical question that can be satisfactorily answered in any useful and general sense.

There are two basic approaches to the problem of nonlinear behavior. The first, entirely mathematical, concerns the behavior of solutions to nonlinear differential equations. Great progress has been made recently in nonlinear dynamical systems; many of the methods and formal results are probably applicable to combustion instabilities, but only limited use has been made of the theory. Two topics in particular are clearly relevant: the theory of subcritical bifurcations, which includes the phenomenon called triggering or nonlinear instability; and the very broad matter of nonlinear behavior with noise.

The second basic aspect of nonlinear behavior is the physical theory of the dominant nonlinear processes. Remarkably little attention has been paid to this subject, other than qualitative descriptive commentary. Yet nonlinear models of physical behavior must be constructed to be consistent with observations if the theoretical work is to produce meaningful results. Nonlinear gasdynamics is always present, is easily modeled accurately, and should therefore always be included in any nonlinear analysis. In liquid rocket engines, observational results suggest, we believe, that in addition to gasdynamics, the dominant nonlinear processes are most probably associated with the fluid mechanics of injected propellants and subsequent spray field. The sensitivity of these processes is enhanced further by supercritical vaporization and combustion processes. Cold-flow tests are a necessary first step, and many have been made, but the influences of large rates of heat addition associated with combustion processes are probably too severe to be ignored.

The general matter of control merits much continued attention. Although the results of passive control devices are fairly well understood, the possible application of active control should be pursued vigorously. This is not simply a matter of wrapping a feedback loop around the system. Intelligent—and therefore successful—use of control will be based on thorough understanding of the available control theory and realistic modeling of the system. Results obtained to date with laboratory devices do not indicate whether active control will be either effective or ineffective. The subject remains in its initial stages.

Acknowledgments

The authors are indebted to Josef M. Wicker for many helpful discussions of feedback loop of combustion instability.

References

[1]Crocco, L., and Cheng, S. I., *Theory of Combustion Instability in Liquid Propellant Rocket Motors,* AGARD monograph, No. 8, Butterworths, London, 1956.

[2]Harrje, D. T., and Reardon, F. H. (eds.), *Liquid Propellant Rocket Combustion Instability,* NASA SP-194, 1972.

[3]Culick, F. E. C., "Combustion Instabilities in Liquid-Fueled Propulsion System—An Overview," AGARD Conf. Proceedings No. 450, 1988.

[4]Culick, F. E. C., and Yang, V., "Prediction of the Stability of Unsteady Motions in Solid Propellant Rocket Motors," *Nonsteady Burning and Combustion Stability of Solid Propellants,* edited by L. Deluca and M. Summerfield, Vol. 143, Progress in Astronautics and Aeronautics, AIAA, Washington, DC, 1992, Chap. 18, pp. 719–780.

[5]Oefelein, J. C., and Yang, V., "Comprehensive Review of Liquid-Propellant Combustion Instabilities in F-1 Engines," *Journal of Propulsion and Power,* Vol. 9, No. 5, 1993, pp. 657–677.

[6]Wicker, J. M., Yoon, M. W., and Yang, V., "Linear and Nonlinear Pressure Oscillations in Baffled Combustion Chambers," *Journal of Sound and Vibration,* Vol. 184, 1995, pp. 141–172.

[7]Elverum, G., Jr., Staudhammer, P., Miller, J., Hoffman, A., and Rockow, R., "The Descent Engine for the Lunar Module," AIAA Paper 67-521, 1967.

[8]Yodzis, C. W., "Engines for Manned Spacecraft," AIAA Paper 68-567, 1968.

[9]Anon, *Liquid Rocket Engine Injectors,* NASA SP-8089, 1976.

[10]Ryan, H. M., Anderson, W. E., Pal, S., and Santoro, R. J., "Atomization Characteristics of Impinging Liquid Jets," *Journal of Propulsion and Power,* Vol. 11, No. 1, 1995, pp. 135–145.

[11]Hsieh, K. C., Shuen, J. S., and Yang, V., "Droplet Vaporization in High-Pressure Environments, I: Near Critical Conditions," *Combustion Science and Technology,* Vol. 76, 1991, pp. 111–132.

[12]Shuen, J. S., Yang, V., and Hsiao, C. C., "Combustion of Liquid-Fuel Droplets at Supercritical Conditions," *Combustion and Flame,* Vol. 89, 1992, pp. 299–319.

[13]Lafon, P., Yang, V., and Habiballah, M, "Pressure-Coupled Vaporization and Combustion Responses of Liquid Oxygen (LOX) Droplets in Supercritical Hydrogen Environments," AIAA Paper 95-2432, 1995.

[14]Yang, V., Hsiao, C. C., Shuen, J. S., and Hsieh, K. C., "Droplet Behavior at Supercritical Conditions," *Recent Advances in Spray Combustion,* edited by K. K. Kuo, Progress in Astronautics and Aeronautics, AIAA, Washington, DC, 1995.

[15]Culick, F. E. C., "High Frequency Oscillations in Liquid Rockets," *AIAA Journal,* Vol. 1, No. 5, 1963, pp. 1097–1104.

[16]Morse, P. M., and Feshback, H., *Methods of Theoretical Physics,* McGraw–Hill, New York, 1953, Chap. 11.

[17]Nickerson, G. R., Culick, F. E. C., and Dang, L. G., "Standard Stability Prediction Method for Solid Rocket Motors," Software and Engineering Associates, Inc., AFRPL TR-83-017, Carson City, NV, 1983.

[18]Rayleigh, Lord, "The Explanation of Certain Acoustical Phenomena," *Royal Institution Proceedings,* Vol. VIII, London, 1878, pp. 536–542.

[19]Rayleigh, Lord, *The Theory of Sound,* Vol. II, Dover, New York, 1945, p. 226.

[20]Culick, F. E. C., "A Note on Rayleigh's Criterion," *Combustion Science and Technology,* Vol. 56, 1987, pp. 159–166.

[21]Zinn, B. T., "Pulsating Combustion," *Advanced Combustion Methods,* edited by F. J. Weinberg, Academic, London, 1986, Chap. 2, pp. 113–181.

[22]Summerfield, M., "A Theory of Unstable Propulsion in Liquid Propellant Rocket Systems," *ARS Journal,* Vol. 21, 1951, pp. 108–114.

[23]Gunder, D. F., and Friant, D. R., "Stability of Flow in a Rocket Motor," *Journal of Applied Mechanics,* Vol. 17, 1950, pp. 327–333.

[24]Heidmann, M. F., and Wieber, P. R., "Analysis of n-Heptane Vaporization in Unstable Combustor with Traveling Transverse Oscillations," NASA TN D-3424, 1966.

[25]Heidmann, M. F., and Wieber, P. R., "Analysis of Frequency Response Characteristics of Propellant Vaporization," NASA TN D-3749, 1966.

[26]Crocco, L., Grey, J., and Harrje, D. T., "Theory of Liquid Propellant Rocket Combustion Instability and Its Experimental Verification," *ARS Journal,* Vol. 30, 1960, pp. 159–168.

[27]Tsien, H. S., "Servo-Stabilization of Combustion in Rocket Motors," *ARS Journal,* Vol. 22, 1952, pp. 256–263.

[28]Ffows-Williams, J. E., "Anti-Sound," *Proceedings of the Royal Society, London,* Vol. A395, 1984, pp. 63–88.

[29]Fung, Y. T., "Active Control of Linear and Nonlinear Pressure Oscillations in Combustion Chambers," Ph.D. Thesis, Dept. of Mechanical Engineering, Pennsylvania State Univ., University Park, PA, 1991.

[30]Fung, Y. T., Yang, V., and Sinha, A., "Active Control of Combustion Instabilities with Distributed Actuators," *Combustion Science and Technology,* Vol. 78, 1991, pp. 217–245.

[31]Yang, V., Sinha, A., and Fung, Y. T., "State Feedback Control of Pressure Oscillations in Combustion Chambers," *Journal of Propulsion and Power,* Vol. 8, No. 1, 1992, pp. 66–73.

[32]Fung, Y. T., and Yang, V., "Active Control of Nonlinear Pressure Oscillations in Combustion Chambers," *Journal of Propulsion and Power,* Vol. 8, No. 6, 1992, pp. 1282–1289.